Renewable Energy 152 (2020) 34–43

Contents lists available at ScienceDirect

Renewable Energy

journal homepage: www.elsevier.com/locate/renene

Transient analysis of a multi-unit pumped storage system during load rejection process

Hao Zhang, Pengcheng Guo*, Longgang Sun

State Key Laboratory of Eco-hydraulic in Northwest Arid Region, Xi'an University of Technology, Xi'an, 710048, Shaanxi, PR China

ARTICLE INFO

Article history:
Received 14 September 2019
Received in revised form
19 November 2019
Accepted 24 December 2019
Available online 25 December 2019

Keywords:
Pumped storage system
Dynamic analysis
Transient process
Transient stability
Renewable power generation

ABSTRACT

Pumped storage systems are attractive for power generation and storage with the development of clean energy. The combined operating mode of wind energy, solar energy and pumped storage systems is an emerging form of energy production, which brings pumped storage systems challenge in transient operation. Here we innovatively present a transient model of a multi-unit pumped storage system by coupling hydraulic system with unit system. We demonstrate that the proposed model can reflect the coupling effect of units during transient process. The simulation is provided with one unit shutdown under three kinds of closing laws and another unit controlled by PID controller at rated condition. The dynamic responses of unit-1 head are negatively related with its flow and output. The fluctuation of the unit-2 head is always higher than that of unit-1, and their fluctuation periods are similar. Analysis of dynamic characteristics of the pumped storage system suggest that transient performance improvement can be achieved by changing the motion law of guide vanes. The influence of guide vanes on the transient performance of the pumped storage system is investigated during load rejection process and the results could enable the flexible operation of multi-unit pumped storage systems for renewable power generation.

1. Introduction

The requirements of energy security and climate change mitigation continue to drive development of renewable energy [1–3]. Clean energy is abundant in sun and wind. The conversion of this energy to rotational mechanical energy, and subsequently to electrical energy, has tremendous potential to power our modern world [4]. Pumped storage station, in which solar energy and wind energy can be transformed and storaged in water, is an effective way of developing and utilizing clean energy [5–7]. The access of solar energy and wind energy, which have strong randomness and volatility, brings challenges to pumped storage stations [8]. They have to change their operating conditions frequently and often run under unrated operating conditions to maintain grid stability [9,10]. This stimulates an interest in transient analysis of pumped storage systems, especially during large fluctuation transient process.

Many scholars have done a lot of research on dynamic modeling and transient analysis of pumped storage systems. For example, Mao et al. [11] studied the stability of pump turbines in view of flow induced noise and they found that the flow induced noise radiation is consistent with internal fluid characteristics. Menendez et al. [12] analyzed the influence of air pressure in the lower reservoir due to the energy losses in the ventilation shafts on the overall energy production and the simulation results show that depending on the usual designs of the ventilation system, the pressure inside the reservoir may vary between 0.67 and 42 (m). Tang et al. [13] proposed an integrated transfer function model for such PSPs in generation mode under primary frequency control and a through time domain sensitivity analysis using both step and realistic load disturbance as inputs was provided. Zhang et al. [14] researched the vibrational performance and its physical origins of a prototype reversible pump turbine in the pumped hydro energy storage power station by experimental study. Zhang et al. [15] investigated the dynamic characteristics of a pump-turbine in S-shaped regions by introducing the nonlinear piecewise function of relative parameters. In previous studies, many scholars focus on the transient modeling and performance improvement of pumped storage systems, in which only a single unit system is considered during transient process. However, the hydraulic system, which has an important effect on the transient performance and stability of a

* Corresponding author.
E-mail address: guoyicheng@xaut.edu.cn (P. Guo).

https://doi.org/10.1016/j.renene.2019.12.111
0960-1481/

Notation

H_r	Rated water head, m
Q_r	Rated turbine flow, m^3/s
f_T	Coefficient of head loss for the common penstock, p.u.
f_{pi}	Coefficient of head loss for the pipe i, p.u.
q_i	Relative flow of the pump turbine i, p.u.
q_T	Relative flow of the common penstock, p.u.
h_s	Relative water head of the bifurcation pipe, p.u.
h_0	Relative static water head of the station, p.u.
Z_T	Normalized value of impedance for the common penstock, p.u.
Z_i	Normalized value of impedance for pipe i, p.u.
α	Water hammer velocity, m/s
A_T	Sectional area of the common penstock, m^2
A_i	Sectional area of the pipe i, m^2
T_T	Elastic time constant of the common penstock, s
T_i	Elastic time constant of pipe i, s
L_T	Length of the common penstock, m
L_i	Length of pipe i, m
x_{1i}	State variable of the pipe i, p.u.
x_{2i}	State variable of the pipe i, p.u.
x_{3i}	State variable of the pipe i, p.u.

pumped storage station, is relatively unexplored. The hydraulic disturbance and coupling effect among units can be described by the hydraulic system and it is complex in the actual project. The hydraulic system has many forms like two units sharing one common penstock, four units with one common penstock and so on [16–19]. Therefore, the coupling between the hydraulic system and pump turbine system of a pumped storage system deserves to be studied.

Motivated by the above discussions, this paper has three advantages which make the approach attractive comparing with the prior works. First, we propose a novel dynamic model framework for a multi-unit pumped storage system considering hydraulic coupling effect among the hydropower units. Second, the effects of hydraulic disturbance and guide vane closing law on transient characteristics of the pumped storage system are investigated by means of numerical simulation. Finally, the results in this paper set the stage for researching the flexible operation of multi-unit pumped storage systems for renewable power generation.

2. System description

In this paper, the multi-unit pumped storage system includes a hydraulic system (a common penstock and branch pipes) and a multi-unit system (pump-turbines, governors and generators) [20]. To illustrate the basic structure and operation mechanism of a multi-unit pumped storage system, the general layout of the multi-unit pumped storage system is presented in Fig. 1.

As shown in Fig. 1, water from upstream reservoir flows into the common penstock and then get into the units through branch pipes. Water flow from branch pipe, which changes with the operating condition of units, drives the runner to rotate. The hydraulic system as a whole, the change of water flow in each branch pipe has coupling effect on the pumped storage system. For example, when one unit suddenly closes its guide vane in the multi-unit pumped storage system, the water flow rate changes accordingly causing the pressure waves in the corresponding pipe. The pressure waves will pass to each unit because of the connectivity of the hydraulic system and they will have an impact on the turbine head, flow of units. This is the hydraulic coupling effect among the units and it becomes more significant during transient process.

Wind energy and solar energy, which have the characteristics of randomness and volatility, cannot satisfy the request of electric power system [21–23]. To connect with power system, they need to operate with pumped storage systems. This combined operation makes the operation conditions of pumped storage systems change frequently. The pumped storage system need to regulate its load dramatically and may conduct bidirectional operation, which brings challenges to pumped storage systems in transient operation [24,25]. How to improve the transient performance of pumped storage systems especially during large fluctuation process urgently needs to be researched. Therefore, the transient analysis of a multi-unit pumped storage system is presented in this paper.

3. Mathematical modeling

3.1. Dynamic characteristics of the hydraulic system

In this paper, we assume that the penstock is long and the elastic water hammer exists in the hydraulic system. To illustrate the effect of hydraulic coupling in a multi-unit pumped storage system, the dynamic characteristics of the hydraulic system considering the elastic water hammer effect in the penstock are shown in Fig. 2.

The base values of the water head and flow are the rated head and rated flow of the pump-turbine (H_r and Q_r). As can be seen from Fig. 2, the hydraulic dynamics of the common penstock can be expressed as [26]:

$$h_s = h_0 - h_{qT} - f_T q_T^2 \tag{1}$$

$$h_{qT} = Z_T q_T \tanh(T_T s) \tag{2}$$

$$q_T = \sum_{i=1}^{n} q_i \tag{3}$$

where h_0, h_s and h_{qT} denote gross head of the pumped storage station, relative head of the bifurcation point and relative head change caused by flow rate in the common penstock, respectively; q_T and q_i are relative flow of the common penstock and i-th pipe, respectively; f_T is head loss coefficient of the common penstock.

The hydraulic dynamics of the i-th pipe can be described as [27]:

$$h_s = h_s - h_{qi} - f_{pi} q_i^2 \tag{4}$$

$$h_{qi} = Z_i q_i \tanh(T_i s) \tag{5}$$

where Z_T and Z_i are the standard value of hydraulic surge impedance in the common penstock and the i-th pipe, respectively; $Z_T = \alpha Q_r/(A_T a_g H_r)$ and $Z_i = \alpha Q_r/(A_i a_g H_r)$; α is the water hammer velocity; A_T and A_i are the sectional area of the penstock and the i-th pipe, respectively; a_g is the gravity acceleration. T_T and T_i denote the elastic time constant of common penstock and i-th pipe, respectively; $T_T = L_T/\alpha$, $T_i = L_i/\alpha$; L_T and L_i are the common penstock length and i-th pipe length, respectively.

For the i-th pipe, its dynamic equation is as follows:

$$h_{qi} = Z_i q_i \tanh(T_i s) \tag{6}$$

Eq. (7) can be obtained by expanding Eq. (6) and omitting the high-order terms.

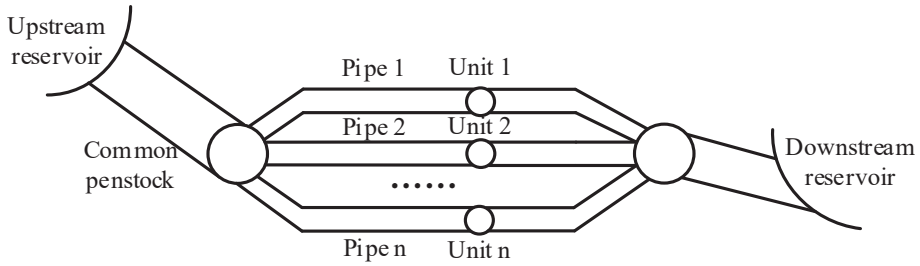

Fig. 1. General layout of a multi-unit pumped storage station.

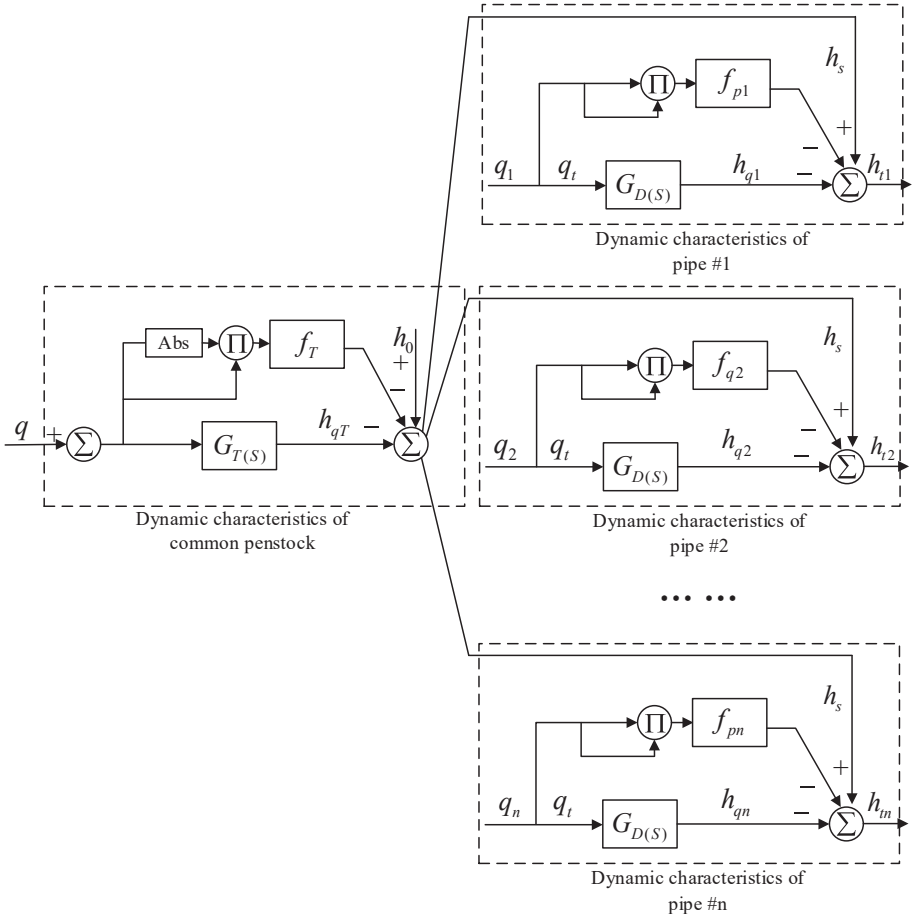

Fig. 2. Dynamic characteristics of the hydraulic system with sharing common penstock and branch pipes.

$$h_{qi}(s) = Z_i \frac{\pi^2 T_i s + T_i^3 s^3}{\pi^2 + 4T_i^2 s^2} q_i(s) \tag{7}$$

Set

$$R(s) = \frac{1}{\pi^2 + 4T_i^2 s^2} q_i(s) \tag{8}$$

Hence, we have

$$h_{q_i}(s) = Z_i \pi^2 T_i R(s) s + Z_i T_i^3 R(s) s^3 \tag{9}$$

According to the initial value theorem of Laplace transform, the Laplace transform can be obtained for Eq. (8) and Eq. (9) [28]:

$$q_i = \pi^2 r(t) + 4T_i^2 r''(t) + q_0 \tag{10}$$

$$h_{qi} = Z_i \pi^2 T_i r'(t) + Z_i T_i^3 r'''(t) \tag{11}$$

Set $x_{1i} = r(t)$, $x_{2i} = r'(t)$ and $x_{3i} = r''(t)$. Then, Eq. (11) can be written as state equations as follows:

$$\begin{cases} \dot{x}_{1i} = x_{2i} \\ \dot{x}_{2i} = x_{3i} \\ \dot{x}_{3i} = -\dfrac{\pi^2}{T_i^2} x_{2i} + \dfrac{1}{Z_i T_i^3} h_{qi} \end{cases} \tag{12}$$

Eq. (12) is the state equation of i-th pipe and subscript i denotes

the i-th pipe.

Further, Eq. (10) can be written as follows:

$$q_i = \pi^2 x_1 + 4T_i^2 x_3 + q_0 \tag{13}$$

The dynamic equation of flow can be obtained by deriving Eq. (12) and combining it with Eq. (13), as follows:

$$\frac{dq_i}{dt} = -3\pi^2 x_2 + \frac{4}{Z_i T_i} h_{qi} \tag{14}$$

In the study of hydraulic system dynamics, the control variable is the turbine flow, and the flow change is achieved by controlling the guide vane opening. Therefore, the servomotor displacement can be introduced using the following constitutive equation [29].

$$q_i = \frac{1}{y_r} y_i \sqrt{h_{ti}} \tag{15}$$

where y_r denotes the per-unit value of servomotor displacement at rated load.

Substituting Eq. (11) into Eq. (8), and we have

$$h_{qi} = h_0 - h_{qT} - f_T q_T^2 - \left(f_{pi} + \frac{y_r^2}{y_i^2}\right) q_i^2 \tag{16}$$

f_{pi} denotes the coefficient of head loss in the i-th pipe; q_i is the relative value of flow in the i-th pipe; h_0 and h_{ti} are the relative value of water head and hydro-turbine head, respectively; Water head H_0 denotes the difference in water level between upstream and downstream; h_{qi} denotes the relative value of head change caused by flow change and $G_{D(S)}$ is the transfer function from flow to head.

Set $x_{4i} = q_i$ and the characteristic equation of the hydraulic system based on Eq. (12) and Eq. (14) can be obtained as:

$$\begin{cases} \dfrac{dx_{1i}}{dt} = x_{2i} \\ \dfrac{dx_{2i}}{dt} = x_{3i} \\ \dfrac{dx_{3i}}{dt} = -\dfrac{\pi^2}{T_i^2} x_{2i} + \dfrac{1}{Z_i T_i^3}\left[h_0 - h_{qT} - f_T q_T^2 - \left(f_{pi} + \dfrac{y_r^2}{y_i^2}\right) x_{4i}^2\right] \\ \dfrac{dx_{4i}}{dt} = -3\pi^2 x_{2i} + \dfrac{4}{Z_i T_i}\left[h_0 - h_{qT} - f_T q_T^2 - \left(f_{pi} + \dfrac{y_r^2}{y_i^2}\right) x_{4i}^2\right] \end{cases} \tag{17}$$

3.2. Dynamic characteristics of the pump turbine

The dynamic equation of the turbine output torque is as follows [30]:

$$\frac{dm_t}{dt} = \frac{1}{e_{qh} T_w}\left[-m_t + e_y y - \frac{e e_y T_w}{T_y}(u - y)\right] \tag{18}$$

where m_t is the relative value of turbine output torque; e is the intermediate variable, $e = e_{qy} e_h / e_y - e_{qh}$; e_{qh} and e_{qy} denote the head and guide vane opening transfer coefficients of turbine flow, respectively; e_h and e_y denote the head and guide vane opening transfer coefficients of turbine torque, respectively; T_w and T_y are the time constant of the penstock and servomotor, respectively; u is the controller output.

The nonlinear second-order model of generator is introduced as follows [31]:

$$\begin{cases} \dfrac{d\delta}{dt} = \omega_0 \omega \\ \dfrac{d\omega}{dt} = \dfrac{1}{T_{ab}}(m_t - m_g - D\omega) \end{cases} \tag{19}$$

where δ is the angle of generator rotor; ω denotes the relative deviation of generator speed, $\omega_0 = 2\pi f_0$; D is the generator damping coefficient and m_g is the load disturbance.

The dynamic characteristics of the hydraulic servosystem with PID controller are shown in Fig. 3.

From Fig. 3, the mathematical equation of the hydraulic servosystem can be obtained as follows:

$$\frac{dy}{dt} = \frac{1}{T_y}(u - y + y_0) \tag{20}$$

where y and y_0 denote the per-unit value and initial per-unit value of servomotor displacement, respectively.

The turbine control system is regulated by the common PID method, and the controller output signal can be obtained as:

$$u = -k_p \omega - \frac{k_i}{\omega_0}\delta - k_d \dot{\omega} \tag{21}$$

where k_p, k_i and k_d denote the proportional, integral and differential coefficients of the PID controller, respectively.

Further based on Eqs. (18)-(21), the dynamic model of the pumped turbine system considering the nonlinear factors of generator rotor can be obtained as:

$$\begin{cases} \dfrac{d\delta}{dt} = \omega_0 \omega \\ \dfrac{d\omega}{dt} = \dfrac{1}{T_{ab}}(m_t - m_g - D\omega) \\ \dfrac{dm_t}{dt} = \dfrac{1}{e_{qh} T_w}\left[-m_t + e_y y - \dfrac{e e_y T_w}{T_y}\left(-k_p \omega - \dfrac{k_i}{\omega_0}\delta - k_d \dot{\omega} - y\right)\right] \\ \dfrac{dy}{dt} = \dfrac{1}{T_y}\left(-k_p \omega - \dfrac{k_i}{\omega_0}\delta - k_d \dot{\omega} - y\right) \end{cases} \tag{22}$$

3.3. Dynamic model of the multi-unit pumped storage system

The multi-unit pumped storage system includes a common penstock, pipes, servo systems and generators of each subsystem. To development the dynamic model of the multi-unit pumped storage system, its frame diagram is presented in Fig. 4.

From Fig. 4, water enters the multi-unit pumped storage system through the common penstock. Then, water from the diversion pipe enters the unit group. The hydraulic coupling exists in the common

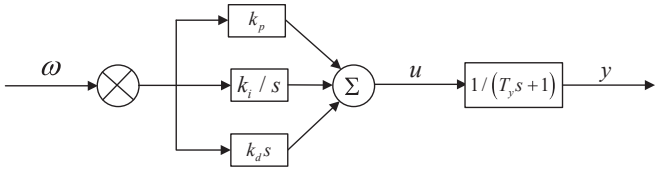

Fig. 3. Dynamic characteristics of the hydraulic servosystem with PID controller.

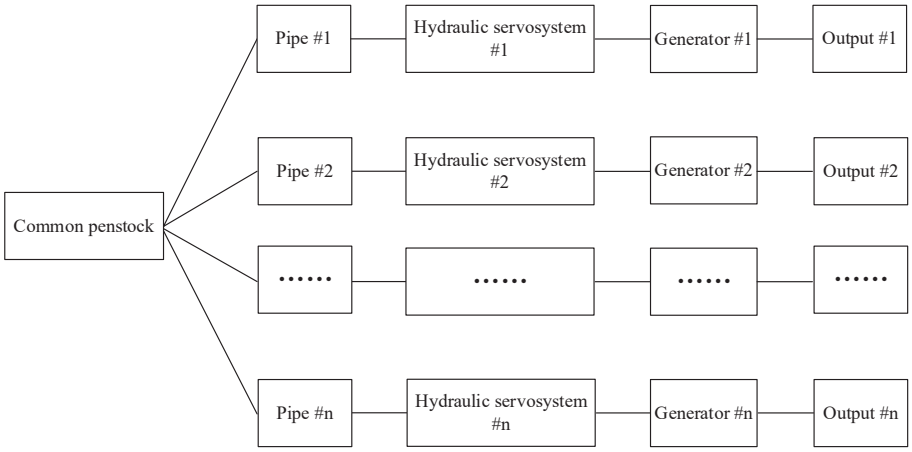

Fig. 4. Frame diagram of the multi-unit pumped storage system.

penstock and the diversion pipes, which means the changes of head and pressure in any one of the diversion pipe can affect the other diversion pipes and the common penstock.

Set $x_{5i} = y$, $x_{6i} = \delta$, $x_{7i} = \omega$, $x_{8i} = m_t$. Eq. (17) is characteristic equation of the hydraulic system and Eq. (22) is the dynamic model of the pump turbine system. The transient model of the multi-unit pumped storage system can be developed by coupling the hydraulic system and the pump turbine system. Therefore, the dynamic model of the multi-unit pumped storage system as shown in Eq. (23) can be obtained by combining Eqs. (17) and (22).

$$
\begin{cases}
\dfrac{dx_{1i}}{dt} = x_{2i} \\
\dfrac{dx_{2i}}{dt} = x_{3i} \\
\dfrac{dx_{3i}}{dt} = -\dfrac{\pi^2}{T_i^2}x_{2i} + \dfrac{1}{Z_i T_i^3}\left[h_0 - h_{qT} - f_T q_T^2 - \left(f_{pi} + \dfrac{y_r^2}{x_{5i}^2}\right)x_{4i}^2\right] \\
\dfrac{dx_{4i}}{dt} = -3\pi^2 x_{2i} + \dfrac{4}{Z_i T_i}\left[h_0 - h_{qT} - f_T q_T^2 - \left(f_{pi} + \dfrac{y_r^2}{x_{5i}^2}\right)x_{4i}^2\right] \\
\dfrac{dx_{5i}}{dt} = \dfrac{1}{T_y}\left[\left(-k_p x_{7i} - \dfrac{k_i}{\omega_0}x_{6i} - k_d\dot{x}_{7i}\right) - x_{5i} + y_0\right] \\
\dfrac{dx_{6i}}{dt} = \omega_0 x_{7i} \\
\dfrac{dx_{7i}}{dt} = \dfrac{1}{T_{ab}}\left(x_{8i} - Dx_{7i} - m_g\right) \\
\dfrac{dx_{8i}}{dt} = \dfrac{1}{e_{qh}T_w}\left[-x_{8i} + e_y x_{5i} - \dfrac{e e_y T_w}{T_y}\left(-k_p x_{7i} - \dfrac{k_i}{\omega_0}x_{6i} - k_d\dot{x}_{7i} - x_{5i}\right)\right]
\end{cases}
\tag{23}
$$

Eq. (23) is the proposed dynamic model of the multi-unit pumped storage system. Parameter i denotes the number of the diversion pipe. Therefore, the dynamic model can reflect the dynamic characteristics of the pumped storage system with several units.

The proposed model is a dynamic model framework of the multi-unit pumped storage system. It means that the model can be used to analyze the transient characteristics of a pumped storage system with different hydraulic system. Moreover, the hydraulic coupling effect among the units can be reflected by the proposed model during transient process and it can also carry out the simulation for the large fluctuation process. The real values of state variable parameters (water head, turbine flow, turbine output) vary widely during transient process and they have different base values. Therefore, when the proposed model uses the real values of state variable parameters, it is difficult to investigate their changing law and dynamic characteristic. To analyze the property and variability of state variable parameters (water head, turbine flow, turbine output) better, they are standardized in the proposed model.

4. Model validation and numerical analysis

To validate the veracity of the proposed dynamic model for multi-unit pumped storage system, simulation test is carried out on a two-unit system during shutdown process ($i = 2$). The numerical results of the nonlinear dynamic model are obtained by Runge-Kutta method, and the system parameters are as follows: rated head $H_r = 640m$; rated speed $n_r = 500rpm$; water hammer wave speed is $1100m/s$; hydraulic surge impedance $Z_T = 1.157$. For the rated operating condition, the values of transfer coefficients and operating parameters are as follows: $e_{qh} = 0.3$, $e_y = 0.4$, $e = -0.15$; $q_0 = 1$, $y_0 = 0.9$, $y_r = 0.9$.

To study the transient characteristics of the two-unit system, the dynamical behaviors of the unit-1 during shutdown process (both units shut down at the same time with guide vane linear closing) are presented in Fig. 5.

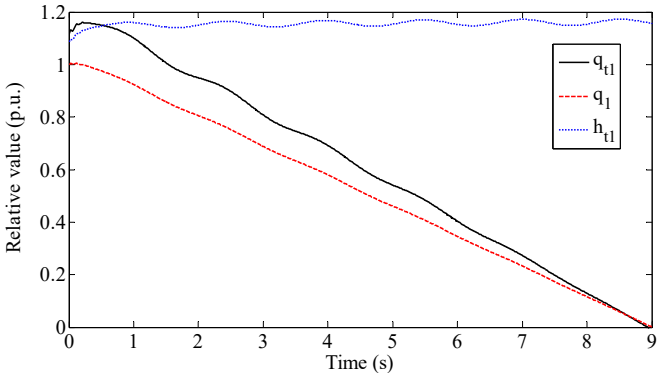

Fig. 5. Dynamic responses of the unit-1 during shutdown process.

For the unit-1, dynamic responses of the relative value of turbine output (q_{t1}), the relative value of turbine flow (q_1) and the relative value of turbine head (h_{t1}) are presented in Fig. 5 during shutdown process. The relative value of turbine flow and turbine output show the similar decreasing trend during the process. The relative value of turbine head fluctuates with the guide vane closing. Note that the relative turbine output experiences a small rise at the beginning of the shutdown and it decreases with fluctuation in the subsequent process. The reason behind this phenomenon is that the $q_{t1} = A_t h_{t1}(q_1 - q_{n1})$ where A_t and q_{n1} denote the turbine gain coefficient and no-load flow. The dynamic responses of the turbine flow, turbine flow and turbine output are consistent with the simulation results in Refs. [27,28]. Therefore, the dynamic characteristics of the unit are rational with guide vane linear closing during shutdown process. Therefore, the simulation test carried out on the two-unit pumped storage system is able to prove that the proposed dynamic model can reflect the dynamic characteristics of the multi-unit pumped storage system during transient process.

To further investigate the coupling effect of the two-unit pumped storage system during transient process, the following simulation experiments are provided with one unit shutdown under different closing laws and another unit controlled by PID controller at rated condition. The PID controller parameters are $k_p = 10, k_d = 5, k_i = 0.1$ and the two units in the diversion pipe have the same characteristic. Assume that both units are operating at rated load and the unit-2 suddenly rejects full load. We assume that the guide vane changes from 0.9 to 0 and the closing speed is constant for different parts. The vanes gradually close from the rated working condition, and the unit-2 flow reduces from rated flow to zero. The guide vane closing law for unit-2 during the shutdown process is presented in Fig. 6.

From Fig. 6, the total time for shutdown process is 9s and there are three kinds of closing laws for unit-2. Law-1 is linear closing and others are folding closing. The specific parameters of the closing law are provided in Table 1.

When the unit-2 has a sudden full load rejection, due to the hydraulic coupling, the head of the unit-1 will be influenced to a certain degree. In order to explore the influence of the three guide vane closing rules of unit-2 on the unit-1 head, the dynamic response of unit-1 head is shown in Fig. 7.

When the unit-2 rejects full load under the three vane closing laws, the dynamic responses of the turbine-1 head are shown in Fig. 7. It can be seen from Fig. 7 that the dynamic responses of the turbine-1 head have a similar increasing trend when unit-2 closes the guide vane under three closing laws. Under the three vane closing rules, the relative values of the turbine-1 head experience a significant increase in the initial stage (0s–1s), and reach the relative maximum value of the head at 0.8s. The relative value of turbine-1 head under guide vane closing law 3 is always higher than that under the other two guide vane closing laws during the adjustment process. Then, under the control of PID controller, the relative value of turbine-1 head shows a gradual upward trend and finally increased to 1.134 at 9s. The fluctuation period is about 1.6s.

It can be seen from the simulation results that the guide vane closing laws of unit-2 have a certain degree of influence on the dynamic response of the turbine-1 head. When the unit-2 closes guide vanes, the flow rate of the water in penstock changes and pressure waves are generated in the hydraulic system. Considering the coupling effect of the hydraulic system, the turbine-1 head will be influenced when pressure waves transfer from unit-2 to unit-1, which results in the fluctuation of turbine-1 head. When the closing speed of unit-2 guide vane increases, the flow rate will change even more dramatically and more significant pressure waves will be generated in the hydraulic system. Therefore, the maximum peak value of the turbine-1 head increases with the closing speed of unit-2 guide vane. Under the three closing laws of unit-2 in this paper, the turbine-1 head fluctuates between 1.143 and 1.085 under the control of the PID controller. Compared with the dynamic responses of the turbine flow and output in the pipe-1 in Figs. 9 and 11, it can be seen that the dynamic responses of the turbine-1 head have a negative correlation with its flow and output, and the fluctuation period is similar.

When the unit-2 suddenly rejects its full load, in order to explore the influence of guide vane closing rules on the turbine-2 head, the following numerical simulation is used to obtain the dynamic responses of the turbine-2 head under different guide vane closing rules, as shown in Fig. 8.

When the turbine in the pipe-2 rejects full load under the three guide vane closing laws, the dynamic responses of the turbine-2 head are shown in Fig. 8. The change of guide vane closing speed can result in the change in flow rate of water in the penstock, which eventually leads to the fluctuation of pressure waves. It can be seen from Fig. 8 that compared with the linear closing law of the guide vane (Law-1), the turbine-2 head has a certain degree of head jump at the turning point under the fold-line closing rules, and then the water head has a similar trend. Because the sudden change in the

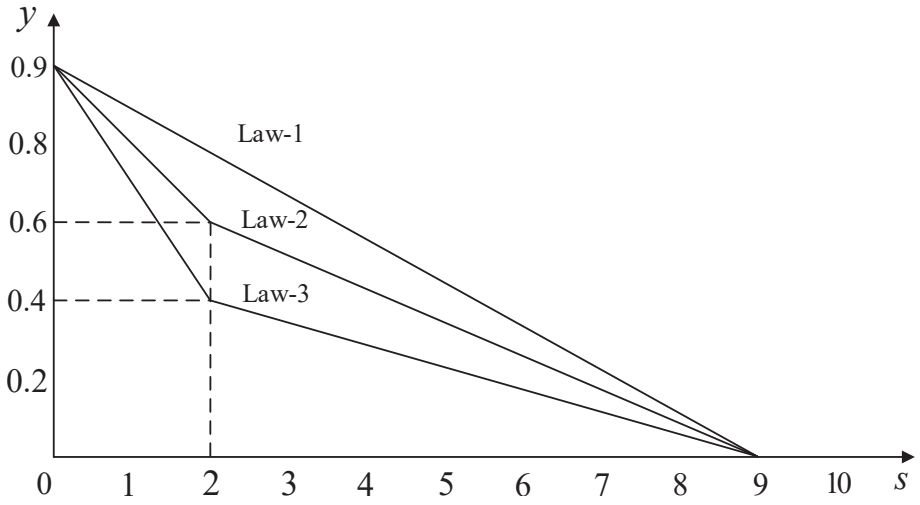

Fig. 6. Closing law of the unit-2 during shutdown process.

Table 1
Closing law of the guide vane with turbine load rejection in split pipe 2.

Closing law	Closing form	Turning point opening(p.u.)	Turning point opening (s)	Total time(s)
Law-1	Linear	no	no	9
Law-2	Folding	0.6	2	9
Law-3	Folding	0.4	2	9

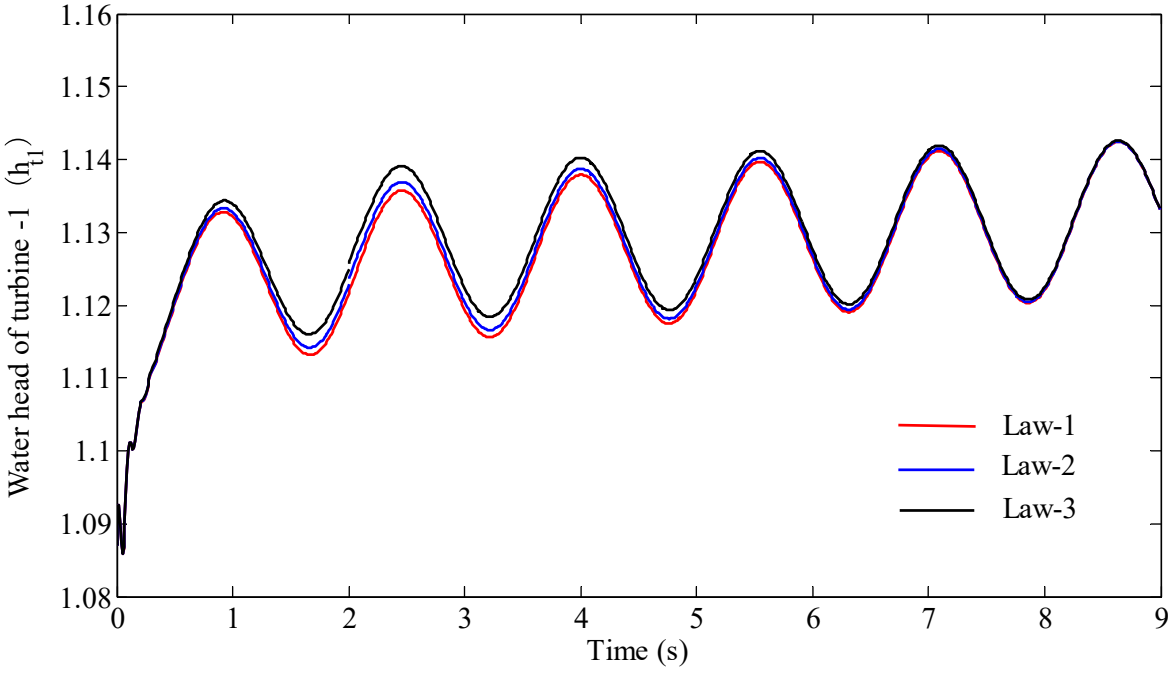

Fig. 7. Dynamic responses of the water head of turbine-1 during shutdown process.

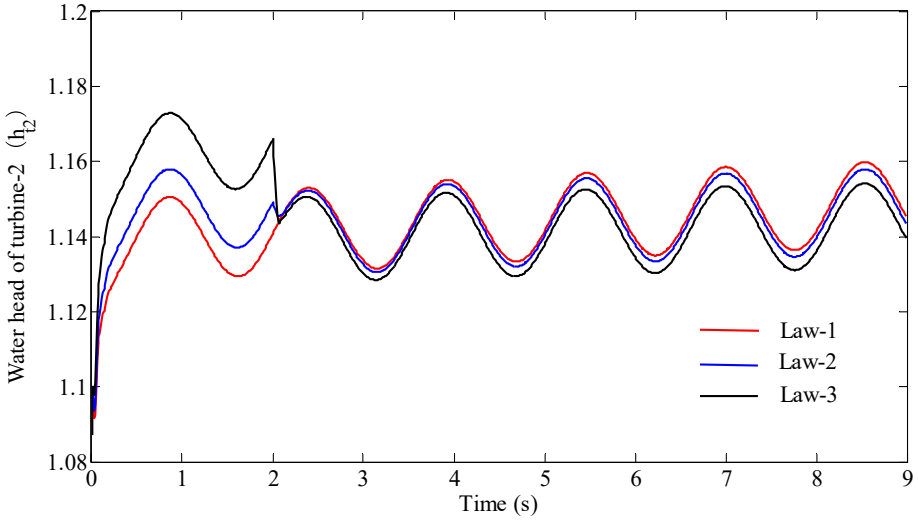

Fig. 8. Dynamic responses of the water head of turbine-2 during shutdown process.

guide vane closing speed at turning point causes the change of flow rate and pressure waves. Under the linear closing law of the guide vane, the relative value of the turbine-2 head is the smallest in the initial stage (0s–1s). The head fluctuation range of the turbine-2 reaches 1.173 in the initial stage with closing law-3. The relative value of the turbine-2 head suddenly decreases 0.02 and 0.006 at the turning point under closing law-2 and law-3, respectively.

The simulation results show that the turbine-2 head is effected significantly by the closing law of guide vanes when the unit-2 rejects full load. Rising rate of turbine-2 head is proportional to the closing rate of guide vanes in the initial stage. The turbine head is characterized by an increase in cyclical fluctuations with the linear closing of guide vanes. The setting of turning point for the guide vane closing law can cause the head jump to different

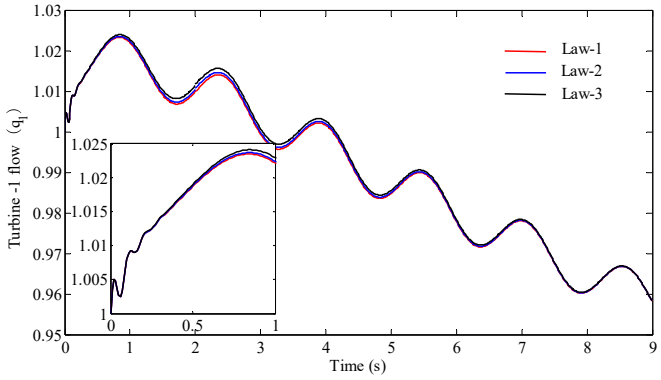

Fig. 9. Dynamic responses of the turbine-1 flow during shutdown process.

degrees, and the setting time of the turning point corresponds to the sudden change of turbine head. Compared to the results in Fig. 7, it can be seen that when the unit-2 rejects full load under the different guide vane closing rules, the fluctuation of the turbine-2 head is always higher than that of the turbine-1, and the fluctuation periods of the turbine head in two units are similar.

In order to study the influence of guide vane closing law on the flow characteristics of turbine-1 when unit-2 rejects full load, dynamic responses of the turbine-1 are investigated under the three guide vane closing laws, and the simulation results are shown in Fig. 9.

When the unit-2 rejects full load under the three guide vane closing laws, the dynamic responses of the turbine-1 flow are shown in Fig. 9. From Fig. 9, the dynamic responses of the turbine-1 flow have a similar changing trend with different guide vane closing laws of unit-2. Under the three guide vane closing rules of unit-2, the relative value of turbine-1 flow fluctuates greatly in the initial stage (0s–1s), and reaches the maximum value at 0.8s. Compared with the closing law 1 and 2, the relative value of turbine-1 flow obtains the maximum rising value (1.024) under the closing law 3. Then the relative value of turbine-1 flow shows a gradual fluctuating reduced trend under the control of the turbine governor PID, and the fluctuation period is about 1.7s. The flow under the three closing laws gradually decreases, and finally reduces to 0.959 at 9s.

According to the simulation results, the guide vane closing law of unit-2 has a certain degree of impact on the turbine-1 flow when unit-2 rejects full load, resulting in fluctuations in the turbine-1 flow. The maximum value of turbine-1 flow increases gradually with the guide vane closing speed of unit-2 increasing. Under the three guide vane closing set of unit-2 in this paper, the maximum rise ratio of the turbine-1 flow is about 0.024 under the control of PID controller.

Further, in order to analyze the variation law of the turbine-2 flow under different vane closing laws when the unit-2 rejects full load, the dynamic responses of the turbine-2 flow are shown in Fig. 10.

When the unit-2 loses full load under the three guide vane closing laws, the dynamic responses of the turbine-2 flow are shown in Fig. 10. From Fig. 10, the dynamic responses of the turbine-2 flow have a similar trend with the corresponding guide vane closing law of unit-2. Under the straight-line closing rule (law 1), the relative value of turbine-2 flow decreases approximately linearly from the initial rated flow to 0, showing small fluctuations during the process. Under the two fold-line closing rules (law 2 and 3), the relative value of turbine-2 flow shows a gradual decreasing trend. For the turning point of guide vane closing law (2s), the guide vane openings of the turning point (0.6 and 0.4) correspond to the relative values of turbine-2 flow 0.76 and 0.43, respectively.

It can be seen from the simulation results that when the turbine-2 loses full load, the changing trend of the turbine-2 flow is closely related to the guide vane closing law, and the flow changing

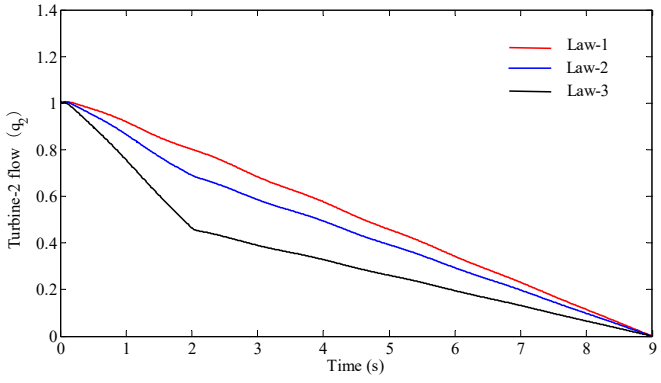

Fig. 10. Dynamic responses of the turbine-2 flow during shutdown process.

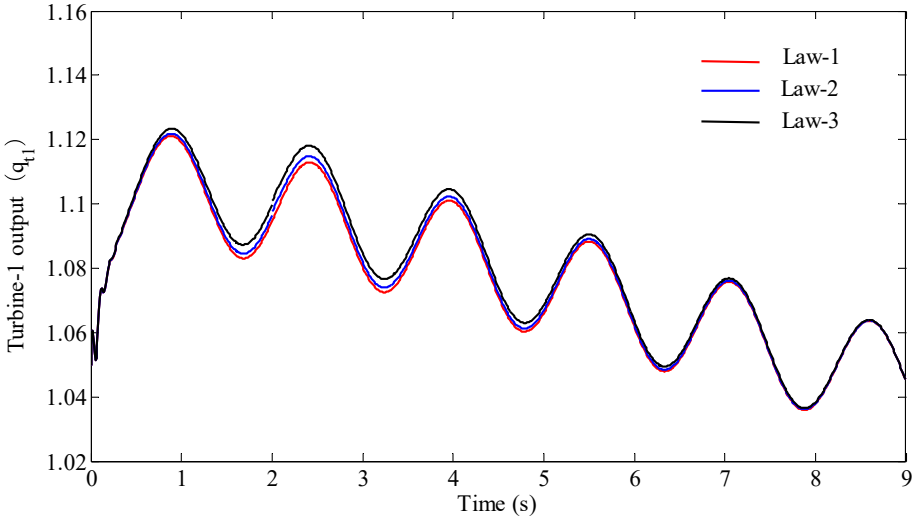

Fig. 11. Dynamic responses of the turbine-1 output during shutdown process.

rate is proportional to the guide vane closing rate. The flow rate of the unit shows an approximate linear decreasing trend with guide vane linear closing. The setting of the guide vane turning point can adjust the transient characteristic of the unit during the load rejection process, and the turning point time corresponds to the sudden change of the unit flow.

During the simulation process, Unit-1 is in the rated working condition and connects to the grid. When the unit-2 suddenly loses full load, investigating its influence on the turbine-1 output is important to the stability study of grid with single tube and two machines. Therefore, under the three guide vane closing laws of unit-2, the dynamic responses of turbine-1 output are shown in Fig. 11.

When the unit-2 rejects full load under the three guide vane closing laws, the dynamic responses of turbine-1 output are shown in Fig. 11. From Fig. 11, the turbine-1 output is influenced to a certain degree with the guide vane of unit-2 closing, and the fluctuation trends of turbine-1 output are consistent with corresponding closing laws. Under the three guide vane closing laws of unit-2, the turbine-1 output shows a large fluctuation in the initial stage (0s–1s), and reaches the maximum output at 0.8s. Compared with the closing laws 2 and 3, the maximum value of the turbine-1 output is the smallest (1.120) under the closing law 1. Then under the control of the PID governor, the relative value of turbine-1 output shows a gradual decreasing trend. The fluctuation period is about 1.6s. The turbine-1 output under the three closing laws gradually decreases, and finally reduces to 1.042 at 9s.

From the simulation results, the guide vane closing laws have a certain degree of impact on the turbine-1 output, when unit-2 loses full load and closes guide vane. Under the three closing laws of the unit-2 guide vanes set in this paper, the maximum rise ratio of turbine-1 output is about 0.122 with the PID control. Compared with the dynamic responses of the turbine-1 flow in Fig. 9, it can be seen that the turbine-1 output has a positive correlation with the dynamic response of its flow, and the fluctuation period is similar.

5. Conclusion and discussion

In this paper, considering the coupling effect of the hydraulic system, a nonlinear dynamic model of the multi-unit pumped storage system is established by combining the hydraulic system and the pump turbine system. The reliability of the proposed model is proved in the process of the two-unit rejecting full load at the same time. Then, the dynamic responses of flow, head and output of each unit are investigated by numerical simulation when one unit rejects full load under three guide vane closing laws. The main conclusions are as follows:

(1) Under the three guide vane closing laws of unit-2 set in this paper, the maximum rise ratio of turbine-1 flow is about 0.024. There is a positive correlation between the dynamic responses of turbine-1 output and flow. The dynamic responses of unit-1 head are negatively related with its flow and output.
(2) The turbine-2 head is significantly affected by the guide vane closing law. The vane closing speed in the initial stage is proportional to the unit head rise speed. The setting time of the turning point corresponds to the sudden change of turbine-2 head. When the unit-2 rejects full load under different vane closing laws, the fluctuation of the turbine-2 head is always higher than that of turbine-1, and their fluctuation periods are similar.
(3) The changing trend of turbine-2 flow is closely related to its guide vane closing law. The flow changing rate is proportional to the closing speed of guide vane. Under the linear closing law of the guide vane, the turbine flow shows an approximate linear decreasing trend. The setting of the turning point can adjust the transient characteristic of the unit during the load rejection process, and the turning point time corresponds to the sudden change of the turbine flow.

The modeling method proposed in this paper provides a theoretical basis for establishing a multi-unit pumped storage system which considers the hydraulic coupling effect of complex hydraulic systems. It provides a reference for studying the transient characteristics and control problems of a multi-unit pumped storage system.

Author contributions section

Hao Zhang: Methodology, Software, Writing- Original draft preparation;

Pengcheng Guo: Conceptualization, Supervision, Investigation, Software, Resources, Writing- Reviewing and Editing;

Longgang Sun: Validation, Visualization.

Declaration of competing interest

The authors declare that they have no conflict of interest concerning the publication of this manuscript.

Acknowledgements

This work was supported by the National Natural Science Foundation of China (Grant number 51839010) and the Shaanxi Provincial Key Research and Development Program (Grant number 2017ZDXM-GY-081).

References

[1] A. Morabito, P. Hendrick, Pump as turbine applied to micro energy storage and smart water grids: a case study, Appl. Energy 241 (2019) 567–579.
[2] Y.N. Zhang, K.H. Liu, H.Z. Xian, X.Z. Du, A review of methods for vortex identification in hydroturbines, Renew. Sustain. Energy Rev. 81 (2018) 1269–1285.
[3] J.Z. Zhou, N. Zhang, C.S. Li, Y.C. Zhang, X.J. Lai, An adaptive takagi-sugeno fuzzy model-based generalized predictive controller for pumped-storage unit, IEEE Access 7 (2019) 103538–103555.
[4] R. Tao, X.Z. Zhou, B.C. Xu, Z.W. Wang, Numerical investigation of the flow regime and cavitation in the vanes of reversible pump-turbine during pump mode's starting up, Renew. Energy 141 (2019) 9–19.
[5] W.C. Guo, J.D. Yang, Dynamic performance analysis of hydro-turbine governing system considering combined effect of downstream surge tank and sloping ceiling tailrace tunnel, Renew. Energy 129 (2018) 638–651.
[6] J.H. Hu, J.D. Yang, W. Zeng, J.B. Yang, Constant-speed oscillation of a pump turbine observed on a pumped-storage model system, J. Fluids Eng.-Trans. ASME 141 (5) (2019), 051109.
[7] D.Y. Zhu, W.C. Guo, Setting condition of surge tank based on stability of hydro-turbine governing system considering nonlinear penstock head loss, Int. J. Electr. Power Energy Syst. 113 (2019) 372–382.
[8] B. Suyesh, V. Parag, D. Keshav, A. Ahmed, O. Abdul-Ghani, Novel trends in modelling techniques of Pelton Turbine bucket for increased renewable energy production, Renew. Sustain. Energy Rev. 112 (2019) 87–101.
[9] B.B. Xu, D.Y. Chen, M. Venkateshkumar, Y. Xiao, Y. Yue, Y.Q. Xing, P.Q. Li, Modeling a pumped storage hydropower integrated to a hybrid power system with solar-wind power and its stability analysis, Appl. Energy 248 (2019) 446–462.
[10] A. Morabito, G.D.E. Silva, P. Hendrick, Deriaz pump-turbine for pumped hydro energy storage and micro applications, J. Energy Storage 24 (2019). UNSP 100788.
[11] X.L. Mao, G. Pavesi, D.Y. Chen, H.S. Xu, G.J. Mao, Flow induced noise characterization of pump turbine in continuous and intermittent load rejection processes, Renew. Energy 139 (2019) 1029–1039.
[12] J. Menendez, J.M. Fernandez-Oro, M. Galdo, J. Loredo, Pumped-storage hydropower plants with underground reservoir: influence of air pressure on the efficiency of the Francis turbine and energy production, Renew. Energy 143 (2019) 1427–1438.
[13] R.B. Tang, J.D. Yang, W.J. Yang, J. Zou, X. Lai, Dynamic regulation characteristics of pumped-storage plants with two generating units sharing common

conduits and busbar for balancing variable renewable energy, Renew. Energy 135 (2019) 1064–1077.
[14] Y.N. Zhang, X.H. Zheng, J.W. Li, X.Z. Du, Experimental study on the vibrational performance and its physical origins of a prototype reversible pump turbine in the pumped hydro energy storage power station, Renew. Energy 130 (2019) 667–676.
[15] H. Zhang, D.Y. Chen, C.Z. Wu, X.Y. Wang, J.M. Lee, K.H. Jung, Dynamic modeling and dynamical analysis of pump-turbines in S-shaped regions during runaway operation, Energy Convers. Manag. 138 (2017) 375–382.
[16] R. Tao, R.F. Xiao, F.J. Wang, W.C. Liu, Improving the cavitation inception performance of a reversible pump turbine in pump mode by blade profile redesign: design concept, method and applications, Renew. Energy 133 (2019) 325–342.
[17] H. Zhang, D.Y. Chen, P.C. Guo, X.Q. Luo, A. George, A novel surface-cluster approach towards transient modeling of hydro-turbine governing systems in the start-up process, Energy Convers. Manag. 165 (2018) 861–868.
[18] Z.W. Zhao, H. Zhang, D.Y. Chen, X. Gao, No-load stability analysis of pump turbine at startup-grid integration process, J. Fluids Eng.-Trans. ASME 141 (8) (2019), 081113.
[19] F. Di Michele, E. Felaco, I. Gasser, A. Serbinovskiy, H. Struchtrup, Modeling, simulation and optimization of a pressure retarded osmosis power station, Appl. Math. Comput. 353 (2019) 189–207.
[20] G. Martinez-Lucas, J.I. Perez-Diaz, M. Chazarra, J.I. Sarasua, G. Cavazzini, G. Pavesi, G. Ardizzon, Risk of penstock fatigue in pumped-storage power plants operating with variable speed in pumping mode, Renew. Energy 133 (2019) 636–646.
[21] X.D. Yu, X.W. Yang, J. Zhang, Stability analysis of hydro-turbine governing system including surge tanks under interconnected operation during small load disturbance, Renew. Energy 133 (2019) 1426–1435.
[22] L.K. Zhang, Q.Q. Wu, Z.Y. Ma, X.N. Wang, Transient vibration analysis of unit-plant structure for hydropower station in sudden load increasing process, Mech. Syst. Signal Process. 120 (2019) 486–504.
[23] X.L. Fu, D.Y. Li, H.J. Wang, G.H. Zhang, Z.G. Li, X.Z. Wei, D.Q. Qin, Energy analysis in a pump-turbine during the load rejection process, J. Fluids Eng.-Trans. ASME 140 (10) (2018) 101107.
[24] W. Gil-Gonzalez, A. Garces, A. Escobar, Passivity-based control and stability analysis for hydro-turbine governing systems, Appl. Math. Model. 68 (2019) 471–486.
[25] L.Y. He, L.J. Zhou, S.H. Ahn, Z.W. Wang, Y. Nakahara, S. Kurosawa, Evaluation of gap influence on the dynamic response behavior of pump-turbine runner, Eng. Comput. 36 (2) (2019) 491–508.
[26] L.K. Zhang, Z.Y. Ma, Q.Q. Wu, X.N. Wang, Vibration analysis of coupled bending-torsional rotor-bearing system for hydraulic generating set with rub-impact under electromagnetic excitation, Arch. Appl. Mech. 86 (2016) 1665–1679.
[27] L.S. Xia, Y.G. Cheng, J.D. Yang, F. Cai, Evolution of flow structures and pressure fluctuations in the S-shaped region of a pump-turbine, J. Hydraul. Res. 57 (2019) 107–121.
[28] Y. Zeng, J. Qian, Y.K. Guo, S.G. Yu, Differential equation model of single penstock multi-machine system with hydraulic coupling, IET Renew. Power Gener. 13 (2019) 1153–1159.
[29] C. Trivedi, M.J. Cervantes, B.K. Gandhi, O.G. Dahlhaug, Transient pressure measurements on a high head model francis turbine during emergency shutdown, total load rejection, and runaway, J. Fluids Eng.-Trans. ASME 136 (12) (2014) 121107.
[30] Y.N. Zhang, T. Chen, J.W. Li, J.X. Yu, Experimental study of load variations on pressure fluctuations in a prototype reversible pump turbine in generating mode, J. Fluids Eng.-Trans. ASME 139 (7) (2017), 074501.
[31] D.Y. Li, Y.L. Qin, Z.G. Zuo, H.J. Wang, S.H. Liu, X.Z. Wei, Numerical simulation on pump transient characteristic in a model pump turbine, J. Fluids Eng.-Trans. ASME 141 (11) (2019), 111101.